Kinetics of Elimination and Addition Reactions in Mixtures of Tri-*n*-Octyl Aluminum and 1-Dodecene

Jeffrey C. Gee* and Ruthann M. Hickox

Chevron Phillips Chemical Company, 1862 Kingwood Drive, Kingwood, Texas 77339

Received February 17, 2006

Trialkyl aluminum compounds have been in commercial use for some time, and their reactions with simple alkenes have been studied in detail. In this paper, we present kinetic data at 95, 140, 150, and 160 °C for the neat liquid-phase reactions of tri-*n*-octyl aluminum and 1-dodecene, showing the emergence of octene, hexadecene, eicosene, and docosene isomers, as well as the isomerization of octenes and dodecenes. We used a comprehensive kinetic model and data from eight experiments to calculate four rate constants and one key equilibrium constant for the system. In addition, we estimated relative rates for a number of other fast reactions in the system and obtained sets of rate constants that accurately reproduced our kinetic data at each temperature. These results permitted us to calculate Arrhenius parameters for the system and therefore predict reaction rates for each reaction in this complex system across a broad range of temperatures and reactant concentrations.

Introduction

Aluminum alkyls are important industrial chemicals commonly used in the manufacture of olefins and olefin polymers. In combination with other compounds, such as $TiCl_4$, they are key components of Ziegler−Natta polymerization catalysts.[1] But on their own, they catalyze other olefin chemistries, such as the oligomerization of ethylene to make linear alpha olefins[2] and the dimerization of linear alpha olefins to make vinylidenes (i.e., 2-alkyl-1-alkenes).[3] These later chemistries typically require temperatures in excess of about 150 °C to proceed at reasonable rates.

This paper focuses on the reactions of aluminum alkyls with linear alpha olefins. A number of transformations are possible. Each aluminum alkyl bond can effectively exchange its alkyl group with an olefin, forming a new aluminum alkyl and releasing a new olefin.

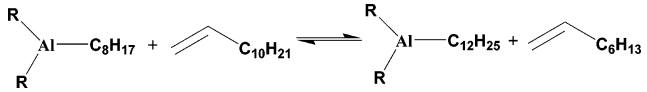

Primary, linear aluminum alkyls can also react with linear alpha olefins in an addition reaction to form a new aluminum alkyl in which the alkyl can be either linear or branched. These new alkyls can eliminate aluminum hydrides to yield either linear internal olefins or vinylidenes; the net effect is the dimerization of an alpha olefin. Other catalysts are also known to effect the same types of dimerizations.[4]

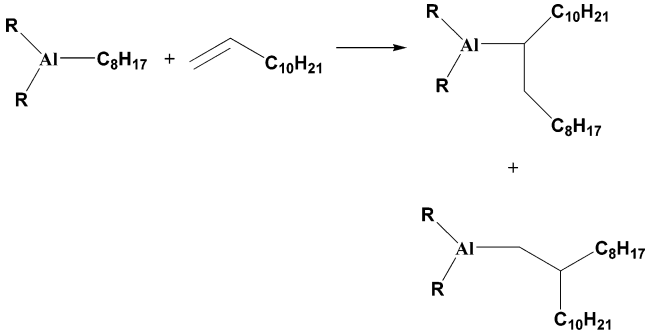

Detectable isomerization of linear alpha olefins to *cis*- and *trans*-2-alkenes (internal olefin) is also possible, and with extended reaction times, further isomerization of 2-alkenes to 3-alkenes occurs.

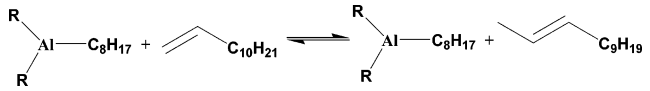

Triethylaluminum (TEA) is a unique case, and it is therefore a common catalyst for the oligomerization of ethylene, because it can undergo linear chain growth by repeated additions of ethylene into the aluminum alkyl bond. Other aluminum species have been shown to catalyze olefin polymerization or oligomerization at relatively mild conditions.[5]

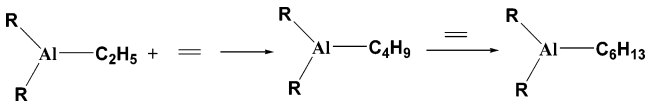

Ziegler and co-workers thoroughly investigated the chemistries of addition and exchange reactions for mixtures of

* Corresponding author. E-mail: geejc@cpchem.com.

(1) Ziegler, Karl; Holzkamp, E.; Breil, H.; Martin, H. *Angew. Chem.* **1955**, *67*, 541. Ziegler, K. German Patent 973,626, 1954. Natta, G.; Pino, P.; Corradini, P.; Danusso, F.; Mantica, E.; Mazzanti, G.; Moraglio, G. *J. Am. Chem. Soc.* **1955**, *77*, 1708. Natta, G. *J. Polym. Sci.* **1959**, *34*, 21. Natta, G.; Pino, P.; Mazzanti, G. *Gazz. Chim. Ital.* **1957**, *87*, 528. Natta, G.; Mazzanti, G.; Valvassori, A.; Sartori, G.; Fumani, D. *J. Polym. Sci.* **1961**, *51*, 411.

(2) Fernald, H.; Gwynn, B.; Kresge, A. (Gulf Research and Development Company, U.S.) U.S. Patent 19693482000, 1969.

(3) Ziegler, K.; Gellert, H.; Zosel, K.; Holzhamp, E.; Schneider, J.; Söll, M.; Kroll, W. *Liebigs. Ann. Chem.* **1960**, *629*, 121.

10.1021/om0601551 CCC: $37.00
Publication on Web 12/06/2006

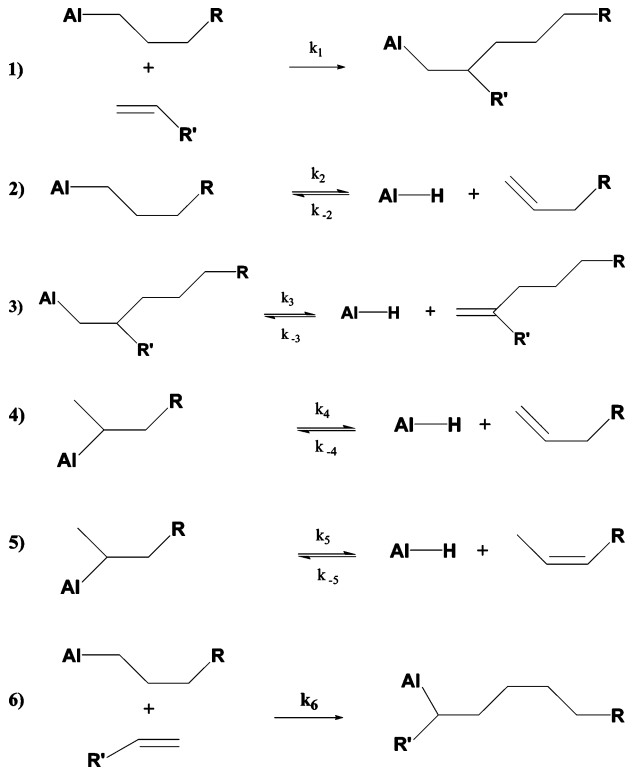

Figure 1. Reactions for a starting mixture of aluminum alkyls and a linear alpha olefin.

aluminum alkyls and a number of olefins.[6] They concluded that aluminum hydride species are intermediates in the exchange reactions and that exchange occurs by elimination followed by addition. Figure 1 illustrates the main reactions expected to occur when an aluminum alkyl with at least four carbons per alkyl group is combined with a linear alpha olefin having at least four carbons; for simplicity, only one alkyl group is shown for each aluminum.

Not all conceivable reactions are included in this list. For example, following reaction 3, we do not include the reaction in which aluminum hydride reacts with a vinylidene to form a tertiary alkyl. Such a species would eliminate to form trisubstituted olefins, which are not observed in these systems. Similarly, we do not observe products expected to form from an addition reaction between a linear alpha olefin (or other olefin) and the branched aluminum alkyl shown in reaction 3, so these reactions are not shown in Figure 1.

There are a number of published reports on the kinetics of these reactions. Based on investigations using diethyl aluminum hydride and a number of olefins, Ziegler reported $k_{-2} \approx 2k_{-3}$,

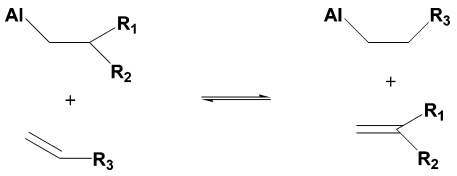

Figure 2. Exchange corresponding to K_{eq}.

and $k_{-5} \approx 0.02k_{-2}$, indicating that the rate of aluminum hydride addition decreases in the order linear alpha olefins > vinylidenes > internal olefins.[7] Ziegler and co-workers also estimated the equilibrium constant at 120 °C for the exchange shown in Figure 2 to be about 40.[6] Therefore, at 120 °C, $K_{eq} = (k_3/k_{-3})/(k_2/k_{-2}) \approx 40$. Egger investigated the elimination of isobutene from triisobutyl aluminum in the gas phase in the presence of excess ethylene, concluding that the elimination was first-order in aluminum alkyl and occurred through a cyclic, four-center transition state.[8]

In addition to the reactions noted in Figure 1, aluminum alkyls also undergo reversible dimerization.[9] Complete dimerization of the aluminum alkyl would effectively reduce by one-third the number of aluminum alkyl bonds available for reactions noted in Figure 1. The aluminum alkyl bonds participating in the bridging bonds of the dimer are no longer available to participate in reactions 1−6.

In this paper, we report the results of our work to estimate values for the 10 rate constants noted in eqs 1−6 at 95, 140, 150, and 160 °C for mixtures of tri-*n*-octyl aluminum (TNOA) and 1-dodecene (C12 NAO) in the liquid phase. We considered models that assumed either complete association of aluminum alkyls into dimers or no association of the aluminum alkyls into dimers. We are not aware of other reports that describe the simultaneous estimation of the rate constants for these elimination and addition reactions. Our goal was to construct a model for the entire system and use one data set to calculate rate constants for as many rate-limiting (or slow) reactions as possible.

In eight separate experiments, we combined TNOA and C12 NAO so that initially the moles of C8 chains and the moles of C12 chains were the same. Because the starting olefin and the starting alkyl group were of different chain lengths, we could easily monitor the exchange, addition, and isomerization reactions using gas chromatography. Extended reaction times gave mixtures containing C8, C12, C16, C20, and C24 products.

As each mixture heated under a nitrogen atmosphere at the target temperature, we periodically withdrew small aliquots of reaction mixture and immediately quenched them in aqueous NaOH solutions for several minutes at 90−95 °C. The quenching reactions converted aluminum alkyls to aluminate salts and paraffins but did not alter the distribution of olefins in the mixtures. (Quenching reactions involving short chain alkyls have reportedly led to some formation of olefin rather than paraffin, but such olefin formation requires temperatures approaching 180−200 °C. Our quenching reactions occurred at temperatures below 100 °C, and we have observed only alkanes and no alkenes when hydrolyzing these type aluminum alkyls in our laboratory.)[10] Using gas chromatography, we analyzed the

(4) Small, B.; Schmidt, R. *Chem.−Eur. J.* **2004**, *10*, 1014. Wu, S.; Shiwei, L. *J. Mol. Catal.* **2003**, *198*, 29. Small, B. *Organometallics* **2003**, *22*, 3178. Wasserscheid, P.; Eichmann, M. *Catal. Today* **2001**, *66*, 309. Small, B.; Marcucci, A. *Organometallics* **2001**, *20*, 5738. Slaugh, L. H.; Schoenthal, G. W. (Shell Oil Company, U.S.) U.S. Patent 19874658078, 1987. Wu, F. (Ethyl Corporation, U.S.), U.S. Patent 19925087788, 1992. Lin, K.; Nelson, G. E.; Lanier, C. W. (Ethyl Corporation, U.S.) U.S. Patent 19904973788, 1990.

(5) Korolev, A.; Ihara, E.; Guzei, I.; Young, V.; Jordan, R. *J. Am. Chem. Soc.* **2001**, *123*, 8291. Kim, J. S.; Wojcinski, L. M.; Liu, S.; Sworen, J. C.; Sen, A. *J. Am. Chem. Soc.* **2000**, *122*, 5668. Cameron, P. A.; Gibson, V. C.; Redshaw, C.; Segal, J. A.; Bruce, M. D.; White, A. J. P.; Williams, D. *Chem. Commun.* **1999**, *18*, 1883. Radzewich, C. E.; Guzei, I. A.; Jordan, R. F. *J. Am. Chem. Soc.* **1999**, *121*, 8673. Coles, M. P.; Swenson, D. C.; Jordan, R. F. *Organometallics* **1997**, *16*, 5183. Coles, M. P.; Jordan, R. F. *J. Am. Chem. Soc.* **1997**, *119*, 8125.

(6) Ziegler, K.; Kroll, W.; Larbig, W.; Steudel, O. *Liebigs Ann. Chem.* **1960**, *629*, 53.

(7) Ziegler, K. *Liebigs Ann. Chem.* **1954**, *589*, 91.

(8) Egger, K. W. *J. Am. Chem. Soc.* **1969**, *91*, 2867.

(9) Smith, M. B. *J. Organomet. Chem.* **1974**, *70*, 13. Smith, M. B. *J. Organomet. Chem.* **1972**, *46*, 211. Smith, M. B. *J. Organomet. Chem.* **1972**, *46*, 31. Smith, M. B. *J. Organomet. Chem.* **1970**, *22*, 273. Smith, M. B. *J. Phys. Chem.* **1967**, *71*, 364.

(10) Philipp, B. J.; Mudry, W. L.; Watson, S. C. *Anal. Chem.* **1973**, *45*, 13, 2298.

organic phases of the quenched mixtures, thus determining compositions of the reaction mixtures at several reaction times. Figure 4 shows example chromatograms of the C8 and C20 products. The C8 and C12 products contained linear alpha and internal olefins, along with linear paraffin. The C16, C20, and C24 products contained vinylidene olefins, methyl alkanes, linear internal olefins, and perhaps some linear paraffin, which coeluted with the linear internal olefins for these chain lengths. The GC data showed not only the carbon number distributions in the product mixtures but also the isomer distributions within each carbon number set. GC data did not show aluminum hydride concentrations directly, but addition of an *n*-tridecane internal standard to the reaction mixtures permitted the calculation of total moles of olefin and paraffin in each mixture, confirming that [Al-H] ≪ [Al-R].

In many kinetic studies, investigators design their experiments so that they can observe the behavior of perhaps just one reactant or product in the system. They may use a large excess of one or more reagents, effectively keeping the concentrations of these species constant throughout a particular experiment and enabling the measurement of the concentration changes of just one reactant. Rate constants are then commonly estimated by measuring slopes of lines (e.g., slope of a plot of ln(concentration) versus time in a first-order system).[11]

In other systems, such as the one we wished to study in this work, a number of reactions occur simultaneously, and several different species are involved. We set out to model the entire system and estimate several rate constants from a common data set. While each of our experiments started with essentially two reagents (tri-*n*-octyl aluminum and 1-dodecene), as reactions proceeded, several other reactive species began to accumulate. The predominant ones were as follows:

Al-(primary C8 alkyl)	(yields *n*-octane upon quenching)
Al-(secondary C8 alkyl)	(yields *n*-octane upon quenching)
1-octene	
2-octenes	
Al-(primary C12 alkyl)	(yields *n*-dodecane upon quenching)
Al-(secondary C12 alkyl)	(yields *n*-dodecane upon quenching)
1-dodecene	
2-dodecenes	
Al-(C16 vinylidene alkyl)	(yields methyl pentadecane upon quenching)
Al-(C16 secondary alkyl)	(yields *n*-hexadecane upon quenching)
C16 vinylidene (2-hexyl-1-decene)	
C16 linear internal olefin	
Al-(C20 vinylidene alkyl)-two types	(yields methyl nonadecane upon quenching)
Al-(C20 secondary alkyl)	(yields *n*-eicosane upon quenching)
C20 vinylidene (2-octyl-1-dodecene and 2-hexyl-1-tetradecene)	
C20 linear internal olefin	
Al-(C24 vinylidene alkyl)	(yields methyl tricosane upon quenching)
Al-(C24 secondary alkyl)	(yields *n*-tetracosane upon quenching)
C24 vinylidene (2-decyl-1-tetradecene)	
C24 linear internal olefin	

Following the general reactions 1−6, we can write the rate equations for the changes in concentration of each of the above species—and for Al−H as well. The differential equations

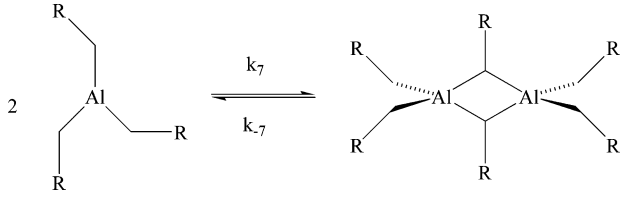

Figure 3. Monomer/dimer equilibrium for aluminum trialkyls.

(excluding reactions for monomer/dimer equilibria of aluminum alkyls for the moment) are shown below:

$$-\mathrm{d[Al\text{-}C8_\alpha]}/\mathrm{d}t = k_1[\mathrm{Al\text{-}C8_\alpha}][\mathrm{C12_\alpha}] + k_1[\mathrm{Al\text{-}C8_\alpha}][\mathrm{C8_\alpha}] + k_2[\mathrm{Al\text{-}C8_\alpha}] - k_{-2}[\mathrm{Al\text{-}H}][\mathrm{C8_\alpha}] + k_6[\mathrm{Al\text{-}C8_\alpha}][\mathrm{C8_\alpha}] + k_6[\mathrm{Al\text{-}C8_\alpha}][\mathrm{C12_\alpha}]$$

$$-\mathrm{d[Al\text{-}C12_\alpha]}/\mathrm{d}t = k_1[\mathrm{Al\text{-}C12_\alpha}][\mathrm{C12_\alpha}] + k_1[\mathrm{Al\text{-}C12_\alpha}][\mathrm{C8_\alpha}] + k_2[\mathrm{Al\text{-}C12_\alpha}] - k_{-2}[\mathrm{Al\text{-}H}][\mathrm{C12_\alpha}] + k_6[\mathrm{Al\text{-}C12_\alpha}][\mathrm{C8_\alpha}] + k_6[\mathrm{Al\text{-}C12_\alpha}][\mathrm{C12_\alpha}]$$

$$-\mathrm{d[C8_\alpha]}/\mathrm{d}t = k_1[\mathrm{Al\text{-}C8_\alpha}][\mathrm{C8_\alpha}] + k_1[\mathrm{Al\text{-}C12_\alpha}][\mathrm{C8_\alpha}] + k_{-4}[\mathrm{Al\text{-}H}][\mathrm{C8_\alpha}] - k_4[\mathrm{Al\text{-}C8_i}] + k_{-2}[\mathrm{Al\text{-}H}][\mathrm{C8_\alpha}] - k_2[\mathrm{Al\text{-}C8_\alpha}] + k_6[\mathrm{Al\text{-}C8_\alpha}][\mathrm{C8_\alpha}] + k_6[\mathrm{Al\text{-}C12_\alpha}][\mathrm{C8_\alpha}]$$

$$-\mathrm{d[C12_\alpha]}/\mathrm{d}t = k_1[\mathrm{Al\text{-}C12_\alpha}][\mathrm{C12_\alpha}] + k_1[\mathrm{Al\text{-}C8_\alpha}][\mathrm{C12_\alpha}] + k_{-4}[\mathrm{Al\text{-}H}][\mathrm{C12_\alpha}] - k_4[\mathrm{Al\text{-}C12_i}] + k_{-2}[\mathrm{Al\text{-}H}][\mathrm{C12_\alpha}] - k_2[\mathrm{Al\text{-}C12_\alpha}] + k_6[\mathrm{Al\text{-}C8_\alpha}][\mathrm{C12_\alpha}] + k_6[\mathrm{Al\text{-}C12_\alpha}][\mathrm{C12_\alpha}]$$

$$-\mathrm{d[Al\text{-}C16v]}/\mathrm{d}t = k_3[\mathrm{Al\text{-}C16v}] - k_{-3}[\mathrm{Al\text{-}H}][\mathrm{C16v}] - k_1[\mathrm{Al\text{-}C8_\alpha}][\mathrm{C8_\alpha}]$$

$$-\mathrm{d[C16v]}/\mathrm{d}t = k_{-3}[\mathrm{Al\text{-}H}][\mathrm{C16v}] - k_3[\mathrm{Al\text{-}C16v}]$$

$$-\mathrm{d[Al\text{-}C20v_a]}/\mathrm{d}t = k_3[\mathrm{Al\text{-}C20v_a}] - k_{-3}[\mathrm{Al\text{-}H}][\mathrm{C20v_a}] - k_1[\mathrm{Al\text{-}C8_\alpha}][\mathrm{C12_\alpha}]$$

$$-\mathrm{d[C20v_a]}/\mathrm{d}t = k_{-3}[\mathrm{Al\text{-}H}][\mathrm{C20v_a}] - k_3[\mathrm{Al\text{-}C20v_a}]$$

$$-\mathrm{d[Al\text{-}C20v_b]}/\mathrm{d}t = k_3[\mathrm{Al\text{-}C20v_b}] - k_{-3}[\mathrm{Al\text{-}H}][\mathrm{C20v_b}] - k_1[\mathrm{Al\text{-}C12_\alpha}][\mathrm{C8_\alpha}]$$

$$-\mathrm{d[C20v_b]}/\mathrm{d}t = k_{-3}[\mathrm{Al\text{-}H}][\mathrm{C20v_b}] - k_3[\mathrm{Al\text{-}C20v_b}]$$

$$-\mathrm{d[Al\text{-}C24v]}/\mathrm{d}t = k_3[\mathrm{Al\text{-}C24v}] - k_{-3}[\mathrm{Al{-}H}][\mathrm{C24v}] - k_1[\mathrm{Al\text{-}C12_\alpha}][\mathrm{C12_\alpha}]$$

(11) For example: Lowry, T. H.; Richardson, K. S. *Mechanism and Theory in Organic Chemistry*, 3rd ed.; Harper and Row: New York, 1987; pp 190−211. Laidler, K. J. *Chemical Kinetics*, 3rd ed.; HarperCollins: New York, 1987.

$$-\mathrm{d[C24v]}/\mathrm{d}t = k_{-3}[\text{Al-H}][\text{C24v}] - k_3[\text{Al-C24v}]$$

$$-\mathrm{d[Al\text{-}C8_i]}/\mathrm{d}t = k_4[\text{Al-C8}_i] - k_{-4}[\text{Al-H}][\text{C8}_\alpha] + k_5[\text{Al-C8}_i] - k_{-5}[\text{Al-H}][\text{C8}_i]$$

$$-\mathrm{d[C8_i]}/\mathrm{d}t = k_{-5}[\text{Al-H}][\text{C8}_i] - k_5[\text{Al-C8}_i]$$

$$-\mathrm{d[Al\text{-}C12_i]}/\mathrm{d}t = k_4[\text{Al-C12}_i] - k_{-4}[\text{Al-H}][\text{C12}_\alpha] + k_5[\text{Al-C12}_i] - k_{-5}[\text{Al-H}][\text{C12}_i]$$

$$-\mathrm{d[C12_i]}/\mathrm{d}t = k_{-5}[\text{Al-H}][\text{C12}_i] - k_5[\text{Al-C12}_i]$$

$$-\mathrm{d[Al\text{-}C16_i]}/\mathrm{d}t = k_5[\text{Al-C16}_i] - k_{-5}[\text{Al-H}][\text{C16}_i] - k_6[\text{Al-C8}_\alpha][\text{C8}_\alpha]$$

$$-\mathrm{d[C16i]}/\mathrm{d}t = k_{-5}[\text{Al-H}][\text{C16}_i] - k_5[\text{Al-C16}_i]$$

$$-\mathrm{d[Al\text{-}C20_i]}/\mathrm{d}t = k_5[\text{Al-C20}_i] - k_{-5}[\text{Al-H}][\text{C20}_i] - k_6[\text{Al-C8}_\alpha][\text{C12}_\alpha] - k_6[\text{Al-C12}_\alpha][\text{C8}_\alpha]$$

$$-\mathrm{d[C20_i]}/\mathrm{d}t = k_{-5}[\text{Al-H}][\text{C20}_i] - k_5[\text{Al-C20}_i]$$

$$-\mathrm{d[Al\text{-}C24_i]}/\mathrm{d}t = k_5[\text{Al-C24}_i] - k_{-5}[\text{Al-H}][\text{C24}_i] - k_6[\text{Al-C12}_\alpha][\text{C12}_\alpha]$$

$$-\mathrm{d[C24_i]}/\mathrm{d}t = k_{-5}[\text{Al-H}][\text{C24}_i] - k_5[\text{Al-C24}_i]$$

$$\begin{aligned}-\mathrm{d[Al\text{-}H]}/\mathrm{d}t = {} & k_{-2}[\text{Al-H}][\text{C8}_\alpha] - k_2[\text{Al-C8}_\alpha] + k_{-2}[\text{Al-H}][\text{C12}_\alpha] - k_2[\text{Al-C12}_\alpha] + k_{-3}[\text{Al-H}][\text{C16v}] - k_3[\text{Al-C16v}] + k_{-3}[\text{Al-H}][\text{C20v}_a] - k_3[\text{Al-C20v}_a] + \\ & k_{-3}[\text{Al-H}][\text{C20v}_b] - k_3[\text{Al-C20v}_b] + k_{-3}[\text{Al-H}][\text{C24v}] - k_3[\text{Al-C24v}] + k_{-4}[\text{Al-H}][\text{C8}_\alpha] - k_4[\text{Al-C8}_i] + \\ & k_{-4}[\text{Al-H}][\text{C12}_\alpha] - k_4[\text{Al-C12}_i] + k_{-5}[\text{Al-H}][\text{C8}_i] - k_5[\text{Al-C8}_i] + k_{-5}[\text{Al-H}][\text{C12}_i] - k_5[\text{Al-C12}_i] + \\ & k_{-5}[\text{Al-H}][\text{C16}_i] - k_5[\text{Al-C16}_i] + k_{-5}[\text{Al-H}][\text{C20}_i] - k_5[\text{Al-C20}_i] + k_{-5}[\text{Al-H}][\text{C24}_i] - k_5[\text{Al-C24}_i]\end{aligned}$$

where $\mathrm{C8_\alpha}$ represents 1-octene; $\mathrm{Al\text{-}C8_\alpha}$ represents a linear, primary C8 aluminum alkyl; $\mathrm{C8_i}$ represents 2-octene; $\mathrm{Al\text{-}C8_i}$ represents a secondary C8 aluminum alkyl; $\mathrm{C12_\alpha}$ represents 1-dodecene; $\mathrm{Al\text{-}C12_\alpha}$ represents a linear, primary C12 aluminum alkyl; $\mathrm{C12_i}$ represents 2-dodecene; $\mathrm{Al\text{-}C12_i}$ represents a secondary C12 aluminum alkyl; C16v represents C16 vinylidene; Al-C16v represents an aluminum alkyl with alkyl being a precursor to C16 vinylidene; $\mathrm{C16_i}$ represents linear internal hexadecenes; $\mathrm{Al\text{-}C16_i}$ represents a secondary C16 aluminum alkyl; $\mathrm{C20v_a}$ represents C20 vinylidene (isomer a); $\mathrm{Al\text{-}C20v_a}$ represents an aluminum alkyl with the alkyl being a precursor to C20 vinylidene (isomer a); $\mathrm{C20v_b}$ represents C20 vinylidene (isomer b); $\mathrm{Al\text{-}C20v_b}$ represents an aluminum alkyl with the alkyl being a precursor to C20 vinylidene (isomer b); $\mathrm{C20_i}$ represents linear internal eicocenes; $\mathrm{Al\text{-}C20_i}$ represents a secondary C20 aluminum alkyl; C24v represents C24 vinylidene; Al-C24v represents an aluminum alkyl with alkyl being a precursor to C24 vinylidene; $\mathrm{C24_i}$ represents linear internal tetracocenes; $\mathrm{Al\text{-}C24_i}$ represents a secondary C24 aluminum alkyl; and Al-H represents aluminum hydride.

We can solve these equations using a numerical approach. A number of numerical methods are known for solving such differential equations, and they typically involve iterative calculations across small time increments.[12] For example, if $-\mathrm{d}A/\mathrm{d}t$ = rate, for a sufficiently small Δt, $-(A_2 - A_1)/\Delta t$ = rate, and $A_2 = -\Delta t(\text{rate}) + A_1$. Successive iterations can give A at any desired time t. The size of Δt obviously has a significant effect on the accuracy of the results, and there are methods available for optimizing its size and minimizing the number of function evaluations required to complete a set of calculations. In our work, we found that the elementary method proposed by Euler and the more sophisticated Runge−Kutta method gave identical results for $\Delta t \leq 0.002$ h. For a given set of k_1, k_2, k_{-2}, k_3, k_{-3}, k_4, k_{-4}, k_5, k_{-5}, and k_6, we could use either method to solve the above equations simultaneously and calculate theoretical concentrations of all reactants in the mixture at any desired time.

For modeling purposes, we chose 10 quantities calculated for each experimental sample. An appropriate set of rate constants therefore had to reproduce not just one experimental curve; it had to reproduce all 10 curves. *Y*-values for the curves were composition data from GC analysis; *X*-values were the reaction times associated with each sample. The *Y*-values for each curve are shown in the list below:

1. % alpha olefin in C8
2. % paraffin in C8
3. % alpha olefin in C12
4. % paraffin in C12
5. % vinylidene in C24 (or C16 or C20)
6. % paraffin in C24 (or C16 or C20)
7. wt % total C8 in mixture
8. wt % total C12 in mixture
9. wt % total C20 in mixture
10. wt % total C24 in mixture

Including the % internal olefins in the C8 and C12 fractions would have been redundant, as those values become fixed once the alpha and paraffin quantities are determined. We observed far less internal olefin than either alpha olefin or vinylidene, so we chose the two most abundant species within each carbon number for our analyses. The distribution curves for C16, C20, and C24 were essentially identical, and we included just one set of distribution curves in the subset of C16/C20/C24. For each time point, we therefore had 10 experimental *Y*-values to use in fitting the rate constants. In each experiment, we collected data on about 25 samples and therefore had about 225 data points in each model.

We used two base models, one that assumed no association of aluminum alkyls into dimers, and one that assumed that essentially all the aluminum (tri) alkyl existed as dimers. In the case of dimers, for any trialkyl aluminum species, the two alkyl groups participating in the bridging bonds were unavailable for elimination or addition reactions. To simplify calculations, the dimer model did not consider dimers having secondary alkyl groups in the bridging bonds; only primary or vinylidene type alkyls were allowed to form bridges. This assumption appeared to be reasonable, because secondary alkyls proved to be of low concentration in our experiments. Eliminating these secondary alkyls greatly reduced the number of possible dimer structures.

In the model that assumed reversible dimerization of aluminum trialkyls, we assumed the extreme case in which the aluminum trialkyls are completely associated into dimers. For the starting concentrations used in our experiments, using $k_7 = 4$ (or 25) and $k_{-7} = 16$ (or 100) effectively established a fast monomer/dimer equilibrium and maintained a 4:1 ratio of

(12) See Chapter 15 of: Press, W. H.; Flannery, B. P.; Teukolsky, S. A.; Vetterling, W. T. *Numerical Recipes in Pascal*; Cambridge University Press: Cambridge, 1986.

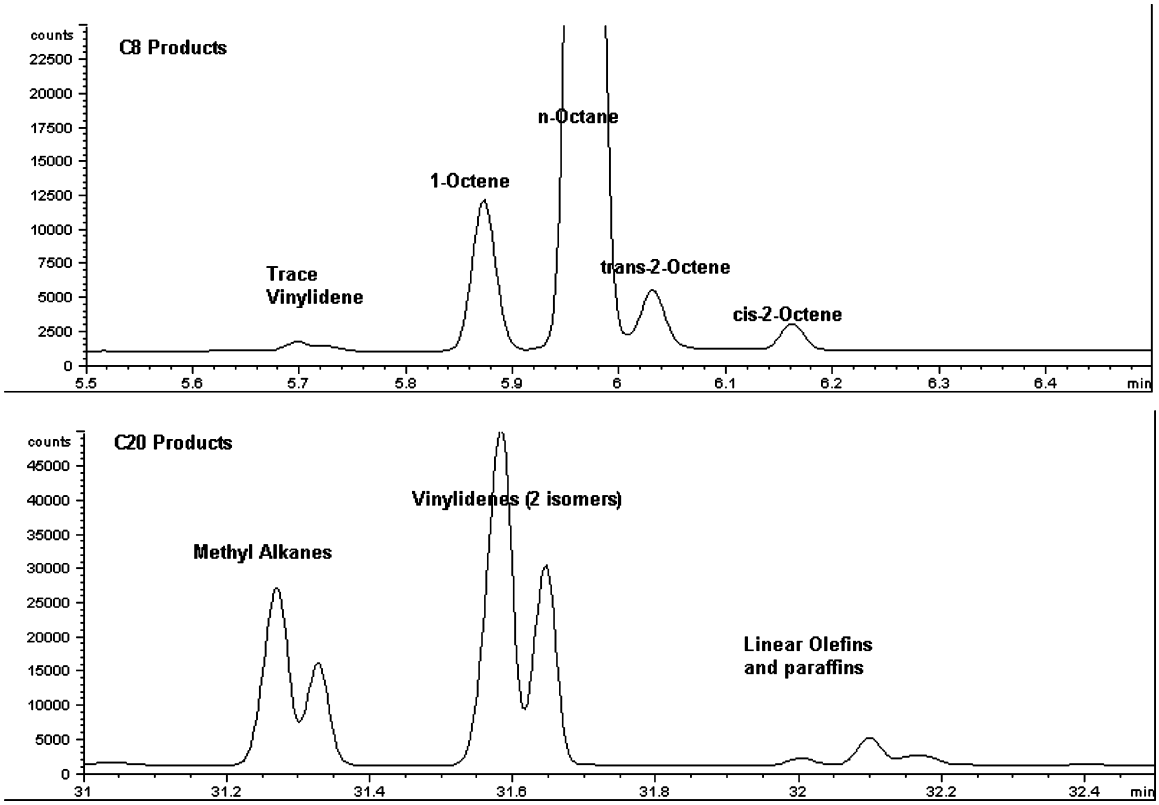

Figure 4. Example chromatograms showing the different types of olefins and paraffins detected in quenched reaction mixtures.

aluminum alkyl species to dimers. To model no dimerization, we assumed $k_7 = 0$. Mathematically, we included dimerization terms analogous to the following:

$$-\mathrm{d[AC8a]}/\mathrm{d}t = 2(k_7[\mathrm{AC8a}][\mathrm{AC8a}]) + k_7[\mathrm{AC8a}][\mathrm{AC12a}] + k_7[\mathrm{AC8a}][\mathrm{AC16v}] + k_7[\mathrm{AC8a}][\mathrm{AC20va}] + k_7[\mathrm{AC8a}][\mathrm{AC20vb}] + k_7[\mathrm{AC8a}][\mathrm{AC24v}] - 2(k_{-7}[\mathrm{D11}]) - k_{-7}[\mathrm{D12}] - k_{-7}[\mathrm{D13}] - k_{-7}[\mathrm{D14}] - k_{-7}[\mathrm{D15}] - k_{-7}[\mathrm{D16}]$$

$$-\mathrm{d[D11]}/\mathrm{d}t = \mathrm{k}_{-7}[\mathrm{D11}] - k_7[\mathrm{AC8a}][\mathrm{AC8a}]$$

where D11 represents dimer formed by bridging between two Al-C8a alkyl bonds; D12 represents dimer formed by bridging between an Al-C8a alkyl bond and an Al-C12a alkyl bond; D13 represents dimer formed by bridging between an Al-C8a alkyl bond and an Al-C16v alkyl bond; D14 represents dimer formed by bridging between an Al-C8a alkyl bond and an Al-C20va alkyl bond; D15 represents dimer formed by bridging between an Al-C8a alkyl bond and an Al-C20vb alkyl bond; and D16 represents dimer formed by bridging between an Al-C8a alkyl bond and an Al-C24v alkyl bond.

There were 21 different dimer species included in the model (D11−D16, D22−D26, D33−D36, D44−D46, D55−D56, and D66).

The aim was to find sets of rate constants that minimized χ-square for both models, where χ-square was given by

$$\sum \frac{(\text{experimental } y - \text{theoretical } y)^2}{(\text{standard error})^2}$$

For a trial set of rate constants, we iteratively solved the rate equations up to the maximum observed reaction time. At each time for which we had experimental points, we used the theoretical concentrations of the individual chemical species to calculate the values we could measure using the GC data. To find the set of rate constants that brought χ-square to a minimum, we used the method of Levenberg−Marquardt.[13] For comparison, we also used the simplex method according to Nelder and Mead.[14]

Results and Discussion

The model of Al-H intermediates appeared to explain the experimental data. For each temperature, we identified sets of rate constants that reproduced the experimental curves quite well (all $R^2 > 0.99$). The two basic models, one assuming all aluminum alkyls to exist in monomer form and one assuming all aluminum trialkyls to exist as dimers, described the experimental data equally well but gave slightly different values for the individual rate constants. Not surprisingly, the model identified some reactions as rate limiting and others as quite fast. Rate constants calculated for the slow reactions appeared to be much more accurately determined than those for the fast reactions. The elimination reactions and the additions of aluminum alkyls with olefins were much slower than the reactions of aluminum hydrides with olefins.

The Levenberg−Marquardt method proved to be superior to the simplex method in minimizing χ-square for this model. Final parameter sets returned by the simplex method generally did not fit experimental data extremely well but were excellent starting points for the Levenberg−Marquardt method, which would return realistic rate constants when given a good set of starting parameters.

(13) See Chapter 14 of: Press, W. H.; Flannery, B. P.; Teukolsky, S. A.; Vetterling, W. T. *Numerical Recipes in Pascal*; Cambridge University Press: Cambridge, 1986.

(14) See Chapter 10 of: Press, W. H.; Flannery, B. P.; Teukolsky, S. A.; Vetterling, W. T. *Numerical Recipes in Pascal*; Cambridge University Press: Cambridge, 1986.

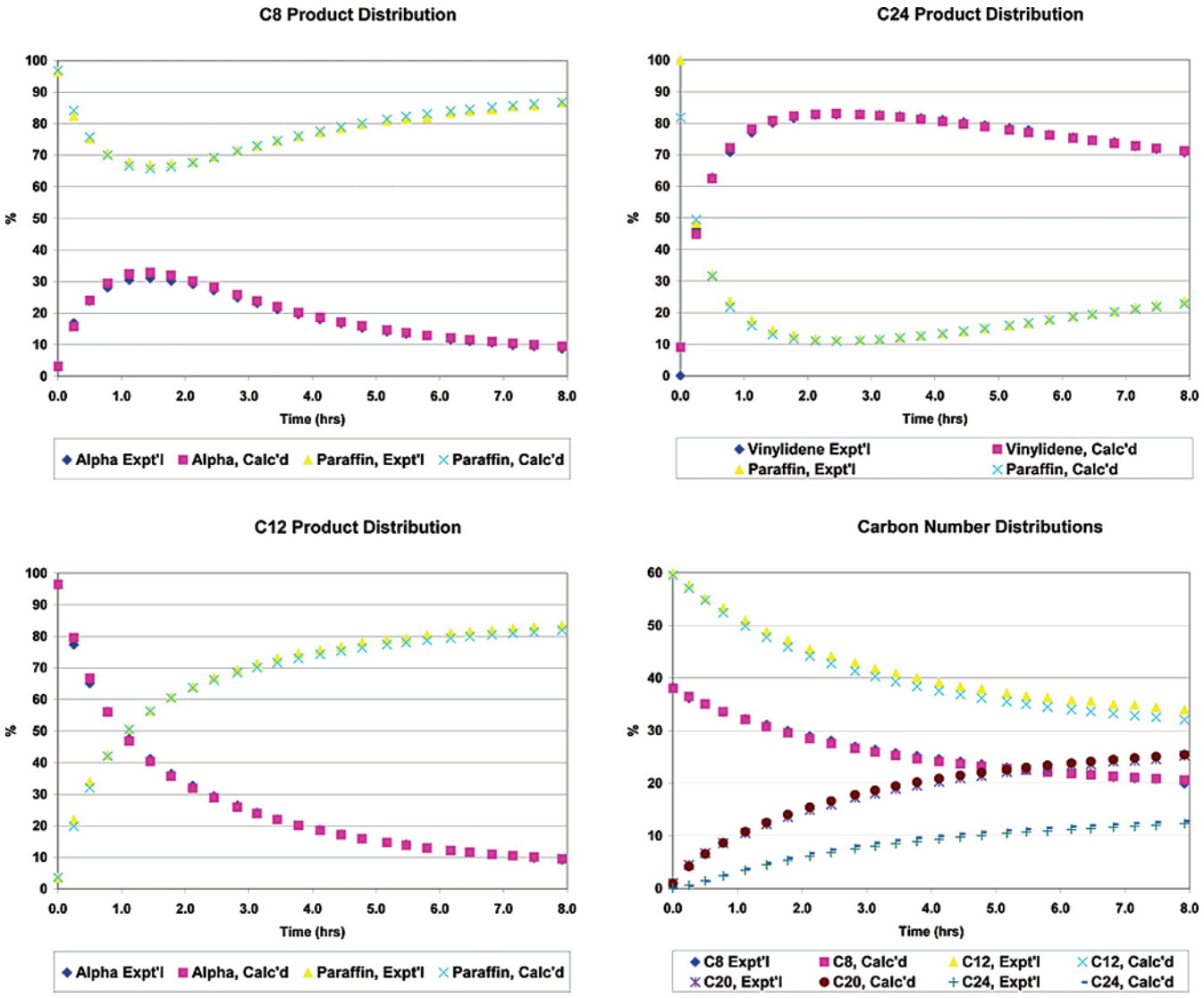

Figure 5. Representative experimental and fitted points for 140 °C.

Multiple fits were required to identify the best sets of rate constants. No fit was successful if all 10 (or 12) rate constants were fit simultaneously. Judicious choices of which parameters to fit and which to hold constant in a given fit eventually led to a good set of fitted parameters. For example, fitting k_2 and k_{-2} simultaneously (or any other pair of forward and reverse rate constants) was never a viable approach. There were too many mathematically equivalent results, and individual rate constants would often increase or decrease by huge, unrealistic values. In practice, we found that the model was not particularly sensitive to the absolute values of the rate constants for the (fast) reactions of aluminum hydride with olefins (i.e., k_{-2}, k_{-3}, k_{-4}, k_{-5}), but that their relative values were important. We generally held k_{-2} fixed at a constant value and performed a number of iterative fits. We could simultaneously fit all k's for the elimination reactions and addition reactions not involving aluminum hydride (k_1, k_2, k_3, k_4, k_5, k_6), then fit k's for all the addition reactions involving aluminum hydride (k_{-3}, k_{-4}, k_{-5}) plus k_1 and k_6. Results would converge after two or three cycles through these loops.

In Figure 5, we present representative graphs showing the experimental and fitted curves for the carbon number distributions, the C8 product distributions, the C12 product distributions, and the C24 product distributions for one experiment at 140 °C. The product distributions for C16 and C20 were essentially like those of C24, and we have omitted those graphs for brevity.

Table 1 summarizes the best fit rate constants determined at the four temperatures for both base models. Reported values are averages of rate constants determined for two separate experiments at each temperature. The table also includes values for $K_{eq} = (k_3/k_{-3})/(k_2/k_{-2})$, which, again, is the equilibrium constant for the exchange shown in Figure 2. A $K_{eq} > 1$ indicates a preference of Al-H to react with and remain bound to linear alpha olefins rather than vinylidenes. The nonlinear correlation coefficients (R^2), which reflect "goodness of fit" for the model, were ≥ 0.99 for all fits.

There were some clear limitations of the model and these experiments. While we could obtain reasonably good fits to our experimental curves, we could determine only some of the 10 rate constants with rather high confidence; for the remaining constants, we could determine only relative values. For example, within each set of best rate constants, we could not determine absolute values for the rate constants describing the reactions of Al-H with any of the olefins (the rate constants denoted with negative subscripts). Within each set of rate constants, if we simultaneously multiply k_{-2}, k_{-3}, k_{-4}, and k_{-5} by any constant >1, the quality of the fitted curves does not change. We therefore could not determine the exact values of these particular

Table 1. Summary of Best Fit Rate Constants and K_{eq}

Assuming Free Aluminum Alkyls				
	95 °C	140 °C	150 °C	160 °C
k_1 (M^{-1} h^{-1})	0.00251 ± 0.00017	0.0741 ± 0.0015	0.109 ± 0.011	0.221 ± 0.0010
k_2 (h^{-1})	0.00251 ± 0.000368	0.654 ± 0.019	1.39 ± 0.70	3.68 ± 0.016
k_{-2} (M^{-1} h^{-1})	125	1000	2000	2000
k_3 (h^{-1})	0.0828 ± 0.00412	7.27 ± 0.70	13.5 ± 6.12	22.8 ± 0.13
k_{-3} (M^{-1} h^{-1})	51.6 ± 16.1	409 ± 29.5	831 ± 63.4	605 ± 10.5
k_4 (h^{-1})	0.389 ± 0.540	45.9 ± 26.7	7.08 ± 0.534	63.5 ± 85.1
k_{-4} (M^{-1} h^{-1})	9.93 ± 5.16	63.9 ± 0.926	40.0 ± 4.29	15.9 ± 8.06
k_5 (h^{-1})	1.33 ± 0.136	58.5 ± 36.1	22.8 ± 21.2	1059 ± 1331
k_{-5} (M^{-1} h^{-1})	578 ± 454	203 ± 35.2	66.4 ± 37.3	221 ± 287
k_6 (M^{-1} h^{-1})	0.000116 ± 0.000028	0.00473 ± 0.00099	0.00811 ± 0.00086	0.0169 ± 0.0011
K_{eq}	79.4 ± 8.80	27.2 ± 0.16	23.4 ± 0.43	20.4 ± 0.33
Assuming Aluminum Alkyls as Dimers				
	95 °C	140 °C	150 °C	160 °C
k_1 (M^{-1} h^{-1})	0.00361 ± 0.00017	0.115 ± 0.0017	0.178 ± 0.018	0.334 ± 0.0033
k_2 (h^{-1})	0.00361 ± 0.000566	1.063 ± 0.036	2.06 ± 0.88	5.60 ± 0.67
k_{-2} (M^{-1} h^{-1})	125	1000	2000	2000
k_3 (h^{-1})	0.110 ± 0.0041	10.1 ± 1.36	19.0 ± 7.65	33.3 ± 3.28
k_{-3} (M^{-1} h^{-1})	28.8 ± 3.68	377 ± 32.1	878 ± 50.7	637 ± 40.6
k_4 (h^{-1})	0.0620 ± 0.0877	8.90 ± 5.12	12.0 ± 1.18	456 ± 67.1
k_{-4} (M^{-1} h^{-1})	26.4 ± 29.2	85.9 ± 1.40	63.7 ± 4.38	18.3 ± 4.36
k_5 (h^{-1})	0.0772 ± 0.0845	7.23 ± 3.38	10.5 ± 0.665	1964 ± 50.8
k_{-5} (M^{-1} h^{-1})	500 ± 707	185 ± 39.8	50.4 ± 3.53	34.5 ± 22.1
k_6 (M^{-1} h^{-1})	0.000315 ± 0.00005	0.00843 ± 0.00088	0.0135 ± 0.00117	0.0253 ± 0.00164
K_{eq}	132 ± 8.80	25.2 ± 0.38	21.0 ± 0.68	18.7 ± 0.81

Table 2. Arrhenius Parameters

Assuming Free Aluminum Alkyls				
	E_a (kJ/mol)	E_a (kcal/mol)	A	Arrhenius r^2
k_1 (M^{-1} h^{-1})	90.9	21.7	2.03×10^{10}	0.998
k_2 (h^{-1})	149	35.7	4.27×10^{18}	0.998
k_3 (h^{-1})	117	28.1	4.00×10^{15}	0.995
k_6 (M^{-1} h^{-1})	101	24.2	2.81×10^{10}	0.999
K_{eq}	−28.4[a]	−6.80	7.34×10^{-3}	0.996
Assuming Aluminum Alkyls as Dimers				
	E_a (kJ/mol)	E_a (kcal/mol)	A	Arrhenius r^2
k_1 (M^{-1} h^{-1})	92.7	22.1	5.20×10^{10}	0.998
k_2 (h^{-1})	151	36.0	9.14×10^{18}	0.997
k_3 (h^{-1})	119	28.4	9.02×10^{15}	0.996
k_6 (M^{-1} h^{-1})	89.4	21.4	1.55×10^{9}	0.999
K_{eq}	−41.6	−10.0	1.57×10^{-4}	0.986

[a] This value is obviously not a formal activation energy, as K_{eq} is an equilibrium constant not a rate constant. But it is mathematically related to the relative activation energies for k_2, k_{-2}, k_3, and k_{-3}.

Table 3. Best Fit Parameters for Simulated Data

	actual set 1	fitted set 1	% error	actual set 2	fitted set 2	% error
k_1	0.108	0.107	−1.0	0.15	0.16	3.6
k_2	0.821	0.825	0.5	0.90	0.95	5.8
k_{-2}	256	1112	334.2	30.0	40.0	33.2
k_3	11.8	11.7	−1.2	13.0	12.2	−6.5
k_{-3}	147	623	323.7	20.0	23.0	15.0
k_4	9.46	32.5	243.7	15.0	23.1	53.8
k_{-4}	6.01	115.7	1825.2	0.50	0.82	64.5
k_5	252	10.8	−95.7	150.0	164.3	9.5
k_{-5}	429	107	−75.1	5.00	9.06	81.2
k_6	0.00704	0.00696	−1.1	0.00900	0.00947	5.2
K_{eq}	25.0	25.2	0.7	21.7	22.2	2.3
	actual set 3	fitted set 3	% error	actual set 4	fitted set 4	% error
k_1	0.090	0.091	1.0	0.02	0.0202	0.9
k_2	0.75	0.76	1.5	0.04	0.0400	0.0
k_{-2}	55.0	88.4	60.8	120	224	86.4
k_3	9.00	9.39	4.3	0.8	0.800	0.0
k_{-3}	30.0	49.1	63.7	50	97.4	94.9
k_4	17.0	34.7	104.1	0.4	0.308	−22.9
k_{-4}	2.00	6.07	203.6	7	13.2	88.9
k_5	5.00	6.98	39.6	1	0.881	−11.9
k_{-5}	2.00	5.65	182.3	45	111	146.3
k_6	0.00200	0.00203	1.6	0.0008	0.000682	−14.8
K_{eq}	22.0	22.2	0.9	48.0	45.9	−4.4

rate constants. However, χ-square dropped rapidly as k_{-2} increased from 100 to 1000 (for temperature = 140−160 °C); further increases in k_{-2} did not affect χ-square significantly, and we kept k_{-2} at 1000 or 2000 for temperatures of 140−160 °C and 125 for 95 °C.

Not surprisingly, the model is sensitive to rate-limiting reactions but not to the fastest ones. The rate-limiting reactions here are clearly the eliminations of Al-H and olefin from aluminum alkyls, as well as the addition reactions of aluminum alkyls with olefins; the reactions of Al-H with alpha olefins and vinylidenes are much faster than the corresponding elimination reactions.

While our gas chromatographic analytical method did not provide a direct measure of the Al-H concentrations in our samples, we could confirm that the concentrations of Al-H were quite small and essentially constant throughout the experiments. By using an *n*-tridecane (i.e., inert) internal standard, we could calculate the total moles of paraffin and olefin in each of the samples. Data confirmed that the total moles of paraffin remained nearly constant throughout each experiment and that the moles of paraffin was about 3 times the moles of TNOA added at the start, consistent with a low, steady-state concentration of Al-H.

Arrhenius plots (ln(k) versus Kelvin temperature) for the 10 rate constants and K_{eq} showed linear behavior for k_1, k_2, k_3, k_6, and K_{eq}. Conversely, plots for the remaining constants were not particularly linear. As k_4 and k_5 relate to behavior of internal olefins (i.e., linear olefins other than alpha olefins), we can perhaps explain the lack of linearity for their Arrhenius plots on the basis of the relatively low concentrations of internal olefins in our experimental samples: Alpha olefins and vinylidenes dominated the olefin populations throughout the experiments, and the model was well suited to determining rate constants for the elimination reactions involving alpha olefins

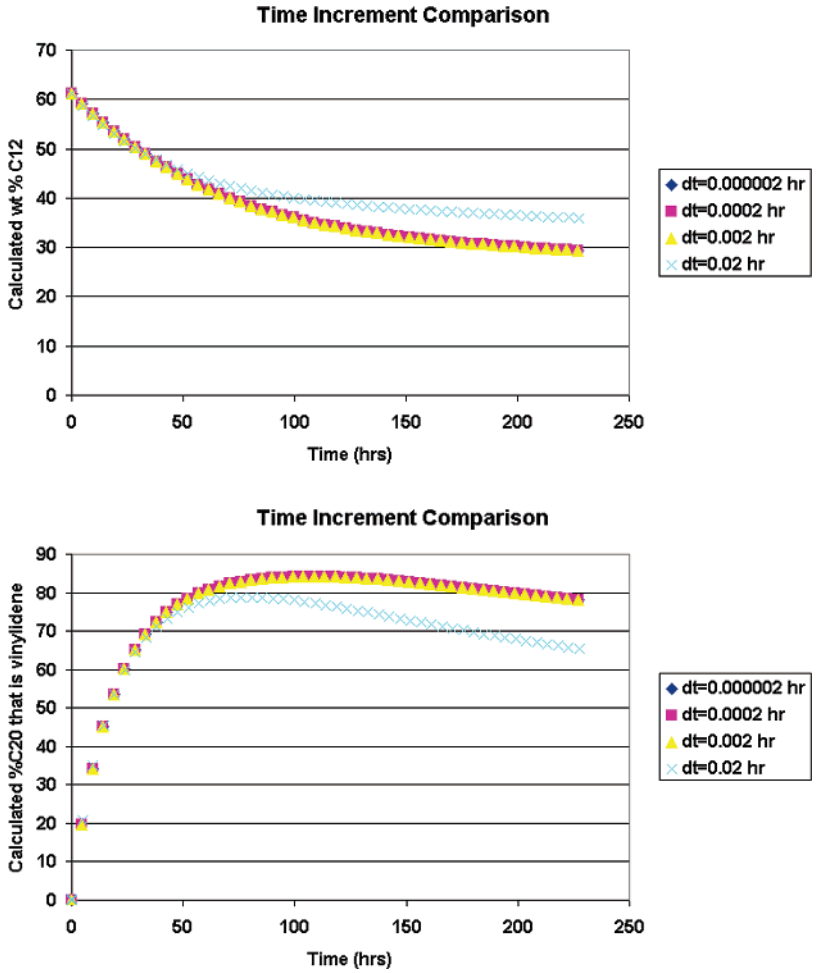

Figure 6. Representative calculations showing effect of time increment. Theoretical curves out to 225 h converge for all dt <0.002 h.

and vinylidenes, as well as rate constants for the addition reactions between aluminum alkyls and olefins. Table 2 summarizes the Arrhenius parameters obtained from our data. The 21.7−22.1 kcal/mol activation energy determined from k_1 for addition of NAO to primary aluminum alkyl is in excellent agreement with the 20 kcal/mol estimate reported for the addition of 1-hexene to triethyl aluminum.[15] Furthermore, the 28.1−28.4 kcal/mol activation energy determined from k_3 for elimination of vinylidenes from aluminum alkyls agrees well with the previously reported 26.6 kcal/mol for elimination of isobutene from tri-isobutyl aluminum.[8]

To estimate the accuracy of the fitting procedure, we applied it to sets of simulated data. Table 3 shows the fitted sets of rate constants alongside the actual sets. All R^2 for fitted sets of curves were >0.99. The procedure generally estimated k_1, k_2, k_3, k_6, and K_{eq} to within 5%, but it failed to estimate the other constants accurately, even though the procedure reproduced the simulated curves. Through K_{eq}, the process accurately determined the relative sizes of k_{-2} and k_{-3}, but a wide range of absolute values for k_{-2} and k_{-3} gave identical values for K_{eq} and fit observed data equally well. In short, a wide range of values for k_{-2}, k_{-3}, k_{-4}, and k_{-5} permit equally good fits to the simulated (or experimental) data, so we could not determine these rate constants with high confidence. The case was similar for k_4 and k_5, and the analyses of simulated data indicate we should have little confidence in the reported values for k_4 and k_5.

The Arrhenius parameters permit calculation of a set of appropriate rate constants for any desired temperature, according to $k = Ae^{(-Ea/RT)}$. However, because the model accurately determines K_{eq} but not necessarily k_{-2} and k_{-3}, we recommend using the Arrhenius parameters to calculate k_3, k_{-3}, k_2, and K_{eq}. Then $k_{-2} = K_{eq}k_2k_{-3}/k_3$. For the model assuming no dimerization of aluminum alkyls, we note that our Arrhenius parameters predict K_{eq} at 120 °C to be 43.6, in close agreement with Ziegler's estimate of 40.[6] For the model assuming complete dimerization of aluminum alkyls, the predicted K_{eq} at 120 °C increases to 53.

Conclusions

The model fit the experimental data well, with R^2 at each temperature exceeding 0.99. From one data set at each temperature, in two separate base models, we determined rate constants for the rate-limiting reactions (k_1, k_2, k_3, and k_6), and we determined the equilibrium constant K_{eq} for the exchange reaction between vinylidene type alkyls and primary, linear alkyls. Rate constants for the fast reactions between aluminum hydride and olefins were difficult to determine accurately, but they are clearly at least 2−3 orders of magnitude larger than the rate constants for the corresponding elimination reactions. Internal olefins were present in only low concentrations, and the rate constants associated with their reactions (k_4, k_{-4}, k_5, and k_{-5}) were not accurately determined from our data. The rate of aluminum hydride reaction with olefins decreases in the order linear alpha olefins > vinylidenes > linear internal olefins. Elimination to form aluminum hydride and olefin occurs faster from vinylidene type alkyls than from linear, primary alkyls and appears to be fastest from secondary alkyls.

(15) Allen, P. E. M. *J. Chem. Soc.* **1963**, 2080.

Experimental Section

Kinetic Experiments. We charged a four-neck, 500 mL round bottomed flask with 1-dodecene, a small amount of *n*-tridecane internal standard, and a stir bar. We fitted the flask with an electronic thermal probe, sealed the necks with rubber septa, and purged the flask with dry nitrogen. In a dry box of nitrogen atmosphere, we charged a 100 mL addition funnel with tri-*n*-octyl aluminum (TNOA) so that the moles of TNOA = 0.33 × moles of 1-dodecene in the flask. Outside the dry box, we fitted the addition funnel to one neck of the flask and heated and stirred the liquid inside the flask to a few degrees below the desired reaction temperature, while maintaining a nitrogen purge for another 30 min. Then we added the TNOA from the addition funnel to the flask and proceeded to maintain the desired reaction temperature using a heating mantle and a J-KEM electronic controller. Periodically, we used a syringe to withdraw about 1 mL of reaction mixture and add it directly to about 5 mL of 20 wt % aqueous NaOH solution in a glass vial. We capped the vial and heated it with agitation to about 95 °C, until the initially formed gel-like mixture had turned to a clear, free-flowing liquid. Once the aqueous and organic phases had separated, we analyzed the organic phase by gas chromatography using an HP 6890 gas chromatograph with a split injector and flame ionization detector. The column was a 50 m × 0.2 mm × 0.5 μm HP-5. The oven temperature began at 40 °C and increased 2.5°/min to 100 °C, then 5°/min to 300 °C, where it remained constant for 12 min.

Starting Concentrations. To calculate starting concentrations for 1-dodecene and Al-*n*-octyl, we calculated densities for mixtures of 1-dodecene and tri-*n*-octyl aluminum at several temperatures. Under a nitrogen atmosphere, we combined a magnetic stir bar, 80.02 g (475 mmol) of 1-dodecene, and 58.11 g (158 mmol) of tri-*n*-octyl aluminum in a 250 mL round bottomed flask. With the flask sealed by a rubber septum, we stirred the mixture and heated it at constant temperature using a heating mantle and J-KEM electronic controller. At a number of temperatures, we used a syringe to quickly withdraw 10.0 mL of liquid, and we determined the mass of the liquid using an electronic balance. Linear least-squares slope and intercept indicated the density of the mixtures as follows: $\rho = -0.000510T + 0.8061$, where T is the temperature in degrees Celcius ($r^2 = 0.96$). The starting molar concentrations of 1-dodecene and Al-*n*-octyl were determined to be about 2.5 M for each temperature we used in our kinetic experiments. During data analysis, we let the computer program adjust these starting concentrations within a window of about 5% around 2.5 M.

T (°C)	density (g/mL)
49.4	0.782
75.3	0.768
89.5	0.761
99.3	0.750
111.3	0.754
119.3	0.744
129.8	0.741

Data Analysis. We analyzed data using a program we wrote with Borland's Delphi compiler. One curve-fitting routine was based on the method according to Levenberg and Marquardt;[13] another routine was based on the simplex method described by Nelder and Mead.[14] Code for the fitting procedures was based on that provided in refs 13 and 14. We did not have multiple samples for each time measurement, so we had no data sets from which to calculate standard errors for our measurements. Data points were therefore equally weighted with the same standard error value of 1. The Euler and Runge−Kutta numerical integration methods gave identical results out to 225 h of reaction time for time increments ≤ 0.002 h. Our fitting procedures used time increments of 0.000002 and 0.002 h in Euler type calculations, obtaining identical results for either time increment. Figure 6 shows some example curves and how they changed with increasing values for the time increment. The curves in Figure 6 were calculated using the best rate constants determined for reactions at 95 °C and starting concentrations of 2.5 M for 1-dodecene and Al-*n*-octyl. Reaction time at this temperature was about 225 h, the longest for any temperature we used.

Acknowledgment. We thank Chevron Phillips Chemical Company for permission to publish this work.

OM0601551